Topological Indices for Open and Thermal Systems Via Uhlmann's Phase

Zhoushen Huang and Daniel P. Arovas
Department of Physics, University of California, San Diego, California 92093, USA
(Received 20 May 2014; published 13 August 2014)

Two-dimensional topological phases are characterized by Thouless-Kohmoto-Nightingale–den Nijs integers, which classify Bloch energy bands or groups of Bloch bands. However, quantization does not survive thermal averaging or dephasing to mixed states. We show that using Uhlmann's parallel transport for density matrices [Rep. Math. Phys. 24, 229 (1986)], an integer classification of topological phases can be defined for a finite generalized temperature T or dephasing Lindbladian. This scheme reduces to the familiar Thouless-Kohmoto-Nightingale–den Nijs classification for $T < T_{c,1}$, becomes trivial for $T > T_{c,2}$, and exhibits a "gapless" intermediate regime where topological indices are not well defined. We demonstrate these ideas in detail, applying them to Haldane's honeycomb lattice model and the Bernevig-Hughes-Zhang model, and we comment on their generalization to multiband Chern insulators.

DOI: 10.1103/PhysRevLett.113.076407 PACS numbers: 71.10.Pm, 03.65.Vf, 03.65.Yz, 73.43.Nq

Introduction.—The discovery of the integer quantum Hall effect and its subsequent theoretical formulation heralded a new paradigm of thinking in condensed matter physics, which has by now blossomed into the rapidly growing field of topological phases [1–3]. In integer quantum Hall systems, the Hall conductance σ_{xy} is an integer multiple C of e^2/h, where C is the first Chern index for the projector onto the filled Bloch bands of the system, as first pointed out in a seminal paper by TKNN [4]. Since an integer cannot change continuously, σ_{xy} is robust against perturbations to the system as long as the bulk energy gap is finite, and is said to be topologically protected. In symmetry-protected topological (SPT) systems, the Chern number itself may vanish by symmetry, but one can still define a topological index, using a restricted set of wave functions (e.g., a subset of bands [5,6], or within a subspace in the Brillouin zone [7], etc.), which remains a nonzero integer, an example being the spin Chern number in quantum spin Hall systems. The Chern number is thus of central importance in the topological characterization of two-dimensional band insulators. Another example is that of topological Floquet systems [8–11], which generally are open systems coupled periodically to an environment, typically idealized as pure eigenstates of the time evolution operator over one period.

Topological classifications and topological phase transitions thus far have been defined for systems at $T = 0$. When dealing with mixed states, such as $T > 0$, quantization is lost. For example, the thermal average of the Chern number would include a contribution from bands not filled at zero temperature, and would no longer be an integer. Any extension of discrete phase classifications to mixed states should be elicited by density matrices [12,13]. Two natural desiderata of such a scheme would be that it reproduce the familiar TKNN or $\mathbb{Z}_2$ classification for pure states, and that it be topologically trivial for $T \to \infty$.

An approach to marrying dephasing in open systems with quantized response functions such as σ_{xy} was developed recently by Avron and collaborators [14], who introduced a notion of compatibility between dissipative and nondissipative evolution of the density matrix in a Lindbladian setting, under which the nondissipative response of the inverse matrix of response coefficients is immune to dephasing. The compatibility condition is highly nongeneric, and below we shall show how dephasing can still allow for a discrete classification of topological phases in a more general setting. Our approach is based on Uhlmann's definition of parallel transport for density matrices [15,16], which maps a cyclic path in a space of density matrices to a matrix M (see Eq. (1) below). The simplest prescription is to examine Uhlmann's phase, $\tilde{\gamma} \equiv \arg[\mathrm{Tr}M]$, which has been studied in the context of quantum information, and may be experimentally measurable [17–20]. Recently Viyuela *et al.* [21] used $\tilde{\gamma}$ to identify topological transitions in one-dimensional fermion systems at finite temperature, where $\tilde{\gamma}$ changes discretely from π to 0 at a critical temperature T_c. For two-dimensional systems, which are the focus of this work, we will compute M at each k_x, and study the spectral flow of its (complex) eigenvalues with respect to k_x. This will be demonstrated in detail using Haldane's honeycomb lattice model [22] and the Bernevig-Hughes-Zhang model [23]. We will briefly comment on its application to more general multiband Chern insulators such as the Hofstadter model [24].

Parallel transport and geometric phases of open systems.—The geometric content over a cyclic path of density matrices can be understood using Uhlmann's parallel transport [15]; see also the Supplemental Material [25]. Consider a cyclic path of density matrices, $\rho_0, \rho_1, \rho_2, \ldots, \rho_N$, with $\rho_a \equiv \rho(\boldsymbol{g}_a)$ where $\boldsymbol{g}_a$ is some parameter vector, e.g., a Bloch momentum, and $\boldsymbol{g}_N = \boldsymbol{g}_0$. Introduce for each ρ_a two matrices W_a and U_a, where W_a is the amplitude and U_a is

unitary, with $W_a = \sqrt{\rho_a}U_a$, hence $\rho_a = W_a W_a^\dagger$. The matrices ρ_a, W_a and U_a are all square and of equal rank. Uhlmann's parallel transport is a protocol for determining the U_a. Two amplitudes W_a and W_b are defined as parallel if the choice of U_a and U_b renders $W_a^\dagger W_b$ a non-negative definite Hermitian matrix. This is equivalent to minimizing the norm $\|W_a - W_b\|$, where $\|A\| = \mathsf{Tr}(A^\dagger A)$. Uhlmann's condition is the analogue of Pancharatnam's parallelity $\langle\psi_a|\psi_b\rangle > 0$ for pure states [26]. The geometric content is contained in $W_0 W_N^\dagger$, which is the mismatch of W_0 with its parallel transported version W_N. This is analogous to the situation *vis-à-vis* pure states, where the Berry phase is encoded in the mismatch between a state before and after a parallel transport, $\exp(i\gamma_{\mathsf{Berry}}) = \mathsf{Tr}(|\psi_0\rangle\langle\psi_N^\dagger|)$ [27,28]. Since we will only be interested in the eigenvalues of $W_0 W_N^\dagger$, it is convenient to introduce 'holonomy matrix' M which has the same eigenvalues as $W_0 W_N^\dagger$,

$$M \equiv \rho_0 U_0 U_N^\dagger = \rho_0 U_{01} U_{12} \cdots U_{N-1N}, \tag{1}$$

where $U_{ab} \equiv U_a U_b^\dagger$. The matrix M is the central object to be considered in the rest of this Letter.

To compute U_{ab}, we note that parallelity allows the polar decomposition $\sqrt{\rho_a}\sqrt{\rho_b} = F_{ab}U_{ab}$, where $F_{ab} = (\sqrt{\rho_a}\rho_b\sqrt{\rho_a})^{1/2}$ is known as the fidelity. Invoking singular value decomposition yields

$$\sqrt{\rho_a}\sqrt{\rho_b} = L_a D_{ab} R_b^\dagger \Rightarrow U_{ab} = L_a R_b^\dagger, \tag{2}$$

where L_a and R_b are unitary matrices. D_{ab} is diagonal (note that a, b do *not* label matrix elements), real, and non-negative, and consists of eigenvalues of F_{ab}. L_a, R_b and D_{ab} all have the same matrix size as ρ_a and ρ_b.

The eigenvalues of M are in general complex, and we write $z_i \equiv r_i e^{i\gamma_i}$ in polar form. We will refer to the phases γ_i as the geometric phases of the path that generates M. This is motivated by the fact that at zero temperature, the holonomy M reduces to a Wilson loop operator whose (nonzero) eigenvalues are the non-Abelian Berry phase factors, see Supplemental Material [25]. Note that these geometric phases are not independent due to the restriction that $\mathsf{det}(M)$ be real and positive, which follows from Eqs. (1) and (2).

Topological characterization of two-dimensional insulators at finite temperature.—We formulate our scheme for general two-dimensional N-band insulators with $L_x \times L_y$ unit cells, assuming translational invariance and periodic boundary conditions in both directions. Let $|\psi_{n\boldsymbol{k}}\rangle$ be the eigenstates of the momentum space Hamiltonian $H_{\boldsymbol{k}}$, where n is the band index and $\boldsymbol{k}$ is the Bloch momentum. At the single particle level, the role of density matrix is played by the correlation matrix

$$\rho_{\boldsymbol{k}} = \textstyle\sum_{n,n'=1}^{N} x_{nn'}(\boldsymbol{k})|\psi_{n\boldsymbol{k}}\rangle\langle\psi_{n'\boldsymbol{k}}|, \tag{3}$$

where $x_{nn'}(\boldsymbol{k})$ are the density matrix elements at each value of $\boldsymbol{k}$. For thermal distributions, we take $\rho_{\boldsymbol{k}} = A_{\boldsymbol{k}} e^{-(H_{\boldsymbol{k}} - \mu N_{\boldsymbol{k}})/T}$, where $\nu \equiv \mathsf{Tr}\rho_{\boldsymbol{k}}$ is the number of filled bands at $T = 0$, independent of $\boldsymbol{k}$. At fixed k_x, one can compute the holonomy $M_{k_x}(\mu, T)$ over the path $k_y \in [0, 2\pi]$. Then as k_x sweeps a 2π cycle, the eigenvalues $\{z_i\}$ trace closed paths in the complex plane. A similar picture emerges when one considers Lindbladian evolution,

$$\dot{\rho} = -\frac{i}{\hbar}[H_0, \rho] + \sum_j C_j \rho C_j^\dagger - \frac{1}{2}C_j^\dagger C_j \rho - \frac{1}{2}\rho C_j^\dagger C_j. \tag{4}$$

With one Lindblad operator $C = \frac{1}{2}\sqrt{\gamma_+}\sigma^+ + \frac{1}{2}\sqrt{\gamma_-}\sigma^-$ connecting two bands, the fixed point of this evolution is $\rho(\infty) = \mathsf{diag}(x, 1-x)$, where $x = \gamma_+/(\gamma_+ + \gamma_-)$. Assuming $\gamma_\pm$ are independent of $\boldsymbol{k}$, the density matrix is equivalent to a thermal one for a flat band model of the type discussed in Ref. [21].

The topological numbers of the system are to be extracted from the winding of the $\{z_i(k_x)\}$. However, we need to take into account that the amplitude spectrum $\{r_i(k_x)\}$ has a gap structure much like that of Bloch spectra. If a particular level $r_i(k_x)$ is isolated from the rest, then one can define a winding number of the corresponding geometric phase, $C_i \equiv [\gamma_i(2\pi) - \gamma_i(0)]/2\pi$. At zero temperature, since M reduces to the Wilson loop operator, C_i reduces to the winding number of the ith non-Abelian Berry phase [29]. For a group of K levels which evolve into each other but remain isolated from the remainder, the topology of the winding is naturally characterized as an element of the K-string braid group on the punctured plane, but there are two natural simple choices. (a) The collective topological number could be the winding number of the sum of the phases, $\sum_{j=1}^{K} \mathsf{arg}(z_j)$. This choice is motivated by the analogy with zero temperature gapless energy bands, where the total Chern number is the winding number of the sum of the individual Berry phases. (b) Alternatively it could also be defined as the winding number of the phase of the sum, $\mathsf{arg}(\sum_{j=1}^{K} z_j)$. Such a choice draws analogy from multipath interference type experiments, where each complex eigenvalue z_i encodes both the weight and the phase of the ith path, and the output is a coherent sum of these complex weights. In both cases, with g spectral gaps in $\{r_i\}$, one obtains $g+1$ topological numbers. For time reversal invariant topological insulators, one should instead consider the time-reversal partner switching similar to that of the non-Abelian Berry phases [7,30,31]. As temperature increases from zero, the gap structure of $\{r_i\}$ also changes, and the system experiences a series of topological transitions until it reaches a fully trivial stage where all topological numbers are zero.

We note that the spectrum of M in Eq. (1) depends on the starting point of the loop. Varying this origin, the general picture of a T-dependent evolution and topological

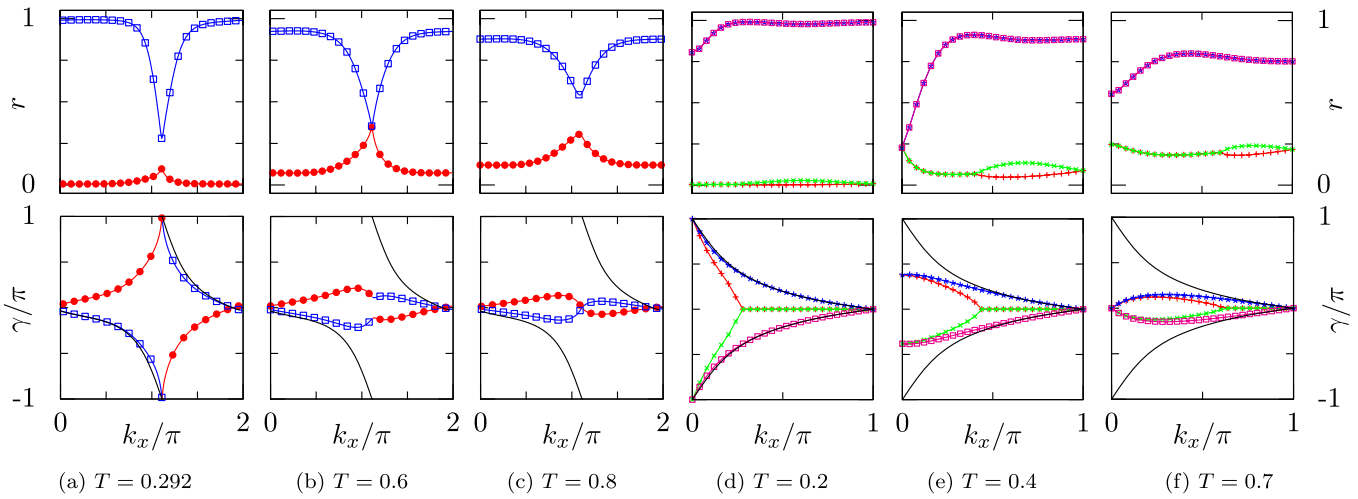

FIG. 1 (color online). Holonomy eigenvalues of the Haldane model (a–c) and the Bernevig-Hughes-Zhang (BHZ) model (d)–(f). Top panels: amplitudes of eigenvalues. Bottom panels: phases of eigenvalues, black solid lines correspond to the Berry phase of the lower band (a)–(c) or the non-Abelian Berry phases of the lower two bands (d)–(f), i.e., the $T = 0$ limit. Color or point type encodes the eigenvalue index. For the Haldane model: in (a), the amplitudes are gapped, and the two phases wind in opposite directions. In (b), the amplitudes are gapless. The phases do not wind. In (c), the amplitudes are gapped again. The phases do not wind. For the BHZ model: The amplitudes are gapped in (d) and (f), but gapless in (e). In the phases, partner switching occurs in (d) but not in (f), see text. Normalization of density matrices is chosen as $\mathrm{Tr}\rho_{\boldsymbol{k}} = \nu$ where ν is the number of filled bands at $T = 0$. Parameters used for Haldane model: $m = 0.5$, $\phi = 0.3\pi$, $t = 0.3$, $\mu = 0.5$. Parameter used for BHZ model: $m = 1.1$, $\Delta = 0.3$, $\mu = 0$. Lattice size: $L_x = 200$, $L_y = 50$.

transitions remains unchanged, although the values of T where transitions occur may vary. One can then define a critical temperature by minimizing $T_c(k_y^0)$ over the loop origin k_y^0. For some models, as we shall see, an origin-independent transition can be defined. Additionally, one also can obtain origin-independent transitions in models of Lindbladian evolution.

Haldane model.—The Haldane model [22] describes electrons hopping on a honeycomb lattice in a fluctuating magnetic field. The model has three parameters t, m, ϕ, where $t \equiv t_{\mathrm{NNN}}/t_{\mathrm{NN}}$ is the ratio of hopping amplitudes between second neighbors and first neighbors, m is the Semenoff mass contrasting the two sublattices, and ϕ is a phase associated with the second neighbor hops which breaks time reversal symmetry. The ground state can be either a Chern insulator (with $C = \pm 1$) or a trivial insulator ($C = 0$) depending on the choice of parameters.

In Figs. 1(a)–1(c), we plot the spectral flow of holonomy eigenvalues (both amplitudes and phases) as functions of k_x, at three different temperatures. Here $k_x \equiv \boldsymbol{k} \cdot \boldsymbol{a}_x$ is the Bloch wave vector along the honeycomb basis vector in the x direction. The matrix M has two eigenvalues for two band models. From $\det M > 0$, the two geometric phases are opposite to each other, and we shall focus on $\gamma_>$, the phase corresponding to the larger eigenvalue magnitude (blue in the figure).

We find that there are three temperature regimes with distinctive spectral patterns. (i) In the low temperature regime (panel a), $\gamma_>$ winds once, and its spectral flow is a minor deviation from the Berry phase flow (i.e., its zero temperature limit). The two amplitudes remain gapped. As T increases, the amplitude gap reduces and the deviation of $\gamma_>$ increases. (ii) In the intermediate temperature regime (panel b), the amplitudes touch and stay gapless. There is no winding in the individual phases. (iii) In the high temperature regime (panel c), the amplitudes are gapped again, and $\gamma_>$ does not wind.

At fixed k_x, the correlation matrices are labeled by the Bloch wave vector along the $\boldsymbol{a}_2$ basis vector of the honeycomb lattice, denoted as $k = \boldsymbol{k} \cdot \boldsymbol{a}_2$. Since these are 2×2 matrices, we can write $\sqrt{\rho_k} = \chi_k[\sqrt{1 - |\boldsymbol{b}_k|^2} + \boldsymbol{b}_k \cdot \boldsymbol{\sigma}]$, implicitly defining χ_k and $\boldsymbol{b}_k$ through Eq. (3). In Fig. 1(b), the k_x point at which the amplitude gap closes, denoted as k_c, coincides with where the π Berry phase occurs. This is the coplanar point, $k_c = \pi + \sin^{-1}(m/6t \sin\phi)$ [32], where the entire path of $\boldsymbol{b}_k$ lies on the same plane that passes through the origin. The winding of $\gamma_>$ over k_x is entirely determined from its value at $k_x = k_c$: it winds once if $\gamma_>(k_c) = \pi$, otherwise it does not wind. The eigenvalues of $M(k_c)$ are

$$z_\pm = \frac{1}{2}\mathrm{Tr}(\rho_0)[\cos(2S) \pm \sqrt{m^2 - \sin^2(2S)}] \qquad (5)$$

with ρ_0 the correlation matrix at $(k_x, k_y) = (k_c, 0)$, and

$$S = \tfrac{1}{2}\left| \oint \boldsymbol{b}_k \times d\boldsymbol{b}_k \right|, \qquad m = \tfrac{f_> - f_<}{f_> + f_<}; \qquad (6)$$

i.e., S is the area enclosed by the path of $\boldsymbol{b}_k$. Here $f_> \geq f_<$ are the two eigenvalues of ρ_0 (i.e., Fermi weights). From Eqs. (5) and (6), we can understand the spectral evolution

as a function of temperature: If $m < |\sin(2S)|$, $z_\pm$ forms a complex conjugate pair, and the amplitude spectrum is gapless; otherwise, they are both real and the amplitudes are gapped. In the gapped regimes, one can check the zero and infinite temperature limits: at $T = 0$, $S = \pi/2$ [33] and $m = 1$, yielding $z_+ = 0$ and $z_- = -1$, hence $\gamma_>(T = 0) = \pi$, whereas for $T \to +\infty$, $m = S = 0$, $z_+ = 1$ and $z_- = 0$, hence $\gamma_>(T \to \infty) = 0$.

As discussed before, in the regime with gapless amplitudes, one has to consider the winding of a collective phase. Using $\tilde{\gamma} \equiv \arg[\mathrm{Tr}M]$ (choice b) and Eq. (5), we have, at $k_x = k_c$, $\exp(i\tilde{\gamma}) = \mathrm{sgn}[\cos(2S)]$. On the other hand, in the gapped regimes, it follows from $\det M > 0$ that $z_\pm$ and hence $\mathrm{Tr}M$ must have the same sign, implying that $\gamma_> = \tilde{\gamma}$ at k_c. Thus one can use $\tilde{\gamma}$ in the entire range of T as *the* geometric phase. The topological index is entirely determined by $\tilde{\gamma}$ at k_c, or equivalently the area S circulated by the path of $\boldsymbol{b}_k$, regardless of the gap structure of the amplitudes—a feature of two band models. Since increasing T generically causes the loop area S to shrink, $\mathrm{sgn}[\cos(2S)]$ must change from $-$ to $+$ and not the other way around. One can thus define a unique transition temperature T_c such that $\tilde{\gamma}(k_c)$ changes discretely from π to 0. The two-dimensional topological transition coincides with the effective one-dimensional transition [21] at k_c. Geometrically, such a topological transition occurs when the loop area S reaches half of its zero temperature value, $S(T_c) = S(0)/2 = \pi/4$. Note that the same critical temperature T_c would be obtained by using $M_a = \rho_a U_a U^\dagger_{a+N}$ for $a \neq 0$, because S is independent of a according to Eq. (6). The transition temperature T_c may depend on other external parameters of the system as well. In Fig. 2, we allow the chemical potential μ to vary, and plot $\mathrm{Tr}M = \cos(2S)$ in the

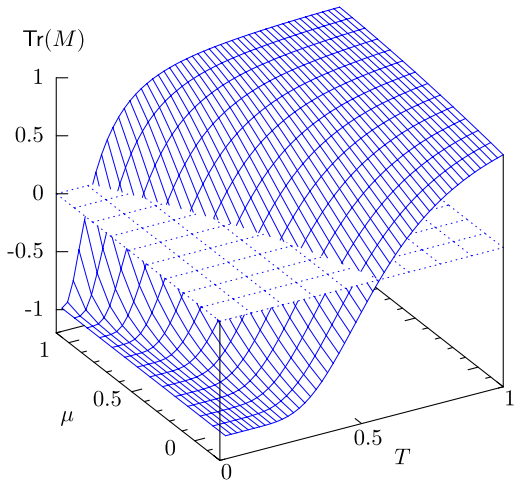

FIG. 2 (color online). $\mathrm{Tr}M$ at $k_x = k_c$ for the Haldane model in the parameter space of temperature T and chemical potential μ. At $k_x = k_c$, $\mathrm{Tr}M$ is real so $\tilde{\gamma}$ depends solely on its sign. A topological transition occurs when $\mathrm{Tr}M$ crosses zero, giving T_c as a function of μ. Other parameters are the same as Fig. 1.

(μ, T) space. $T_c(\mu)$ is determined as the curve at which $\cos(2S)$ crosses zero. For Lindbladian evolution, the area is $S(x) = \pi/4(1-2\sqrt{x(1-x)})$, and setting $S(x_c) = \frac{1}{2}S(0)$ we obtain $x_{c,\pm} = \frac{1}{2} \pm \sqrt{3}/4$. Our result for $x_{c,+}$ corresponds to T_c in Ref. [21]'s analysis of the flat band case. We note that $x = \frac{1}{2}$ corresponds to $T = \pm\infty$, with $x < \frac{1}{2}$ a regime of negative temperature.

BHZ model.—We briefly discuss the BHZ model [23] as an example of the $\mathbb{Z}_2$ class. The Hamiltonian is $H = \sin k_x \sigma_z \tau_x + \sin k_y \tau_y + (2 - m - \cos k_x - \cos k_y)\tau_z + \Delta\sigma_y\tau_y$, with $\Delta \neq 0$ breaking inversion symmetry. The parameters are chosen so that it is in the topological phase at zero temperature. In Fig. 1(d)–(f), we plot its holonomy spectrum in the half-Brillouin zone. The four amplitudes form two pairs (partners), which are gapless for intermediate T but gapped for both low and high T. In the low temperature regime (d), each pair of the geometric phases exhibit partner switching [7,30] where they change from π at $k_x = 0$ to 0 at $k_x = \pi$; hence, the system is topological. After going through the gapless regime (e), the system becomes trivial in the high temperature gapped regime (f) where there is no partner switching.

Conclusion and discussion.—In this work, we introduced a topological characterization of two-dimensional band insulators described by mixed states, resulting from thermal and/or dephasing effects. The classification is in terms of the winding of geometric phases defined through Uhlmann's parallel transport of density matrices. For Haldane's honeycomb lattice model, we found three phases: (i) a low-temperature topological phase classified by the familiar TKNN integers, (ii) a "gapless" intermediate phase, and (iii) a topologically trivial high temperature phase. We found a similar structure in the BHZ model *vis-à-vis* partner switching which defined $\mathbb{Z}_2$ quantum numbers. An analogous procedure works for multiband Chern insulators as well [31], where there is a series of topological transitions induced by changes in the gap structure of the amplitude spectrum.

While our primary interest is an extension of topological indices from pure states to mixed states, we note that it should be experimentally relevant as well [17,18,20,21]. In the context of band insulators, there already exist experimental techniques to measure Berry phases in one dimension [34] and Chern numbers in two dimensions [35]. Such techniques can be extended to measure the Uhlmann phase $\tilde{\gamma} = \mathrm{Tr}M$ through the so-called purification procedure [17], where the amplitude matrix W of a mixed state is mapped to a pure state in an enlarged system, the reduced density matrix of which is the mixed state. The Uhlmann phase $\tilde{\gamma}$ of the mixed state is identified with the Berry phase of the enlarged system, and is thereby measurable. The design and implementation of an adiabatic protocol to measure the Uhlmann phase winding and associated phase transitions of the types discussed here remains a tantalizing possibility.

We are grateful to J. McGreevy, C. Wu, E. Demler, and Da Wang for discussions. Recently, we learned of similar results by Viyuela, Rivas, and Martin-Delgado [36]. We thank O. Viyuela for correspondence. This work was supported by the NSF through Grant No. DMR-1007028 and by the UC Academic Senate.

[1] B. A. Bernevig and T. L. Hughes, *Topological Insulators and Topological Superconductors* (Princeton University Press, Princteon, NJ, 2013).
[2] M. Z. Hasan and C. L. Kane, Rev. Mod. Phys. **82**, 3045 (2010).
[3] X.-L. Qi and S.-C. Zhang, Rev. Mod. Phys. **83**, 1057 (2011).
[4] D. J. Thouless, M. Kohmoto, M. P. Nightingale, and M. den Nijs, Phys. Rev. Lett. **49**, 405 (1982).
[5] D. N. Sheng, Z. Y. Weng, L. Sheng, and F. D. M. Haldane, Phys. Rev. Lett. **97**, 036808 (2006).
[6] E. Prodan, Phys. Rev. B **80**, 125327 (2009).
[7] L. Fu and C. L. Kane, Phys. Rev. B **74**, 195312 (2006).
[8] P. Leboeuf, J. Kurchan, M. Feingold, and D. P. Arovas, Phys. Rev. Lett. **65**, 3076 (1990).
[9] T. Kitagawa, E. Berg, M. Rudner, and E. Demler, Phys. Rev. B **82**, 235114 (2010).
[10] N. H. Lindner, G. Refael, and V. Galitski, Nat. Phys. **7**, 490 (2011).
[11] Z. Gu, H. Fertig, D. P. Arovas, and H. A. Auerbach, Phys. Rev. Lett. **107**, 216601 (2011).
[12] O. Viyuela, A. Rivas, and M. A. Martin-Delgado, Phys. Rev. B **86**, 155140 (2012).
[13] A. Rivas, O. Viyuela, and M. A. Martin-Delgado, Phys. Rev. B **88**, 155141 (2013).
[14] J. E. Avron, M. Fraas, G. M. Graf, and O. Kenneth, New J. Phys. **13**, 053042 (2011).
[15] A. Uhlmann, Rep. Math. Phys. **24**, 229 (1986).
[16] M. Hübner, Phys. Lett. A **179**, 226 (1993).
[17] M. Ericsson, A. K. Pati, E. Sjöqvist, J. Brännlund, and D. K. L. Oi, Phys. Rev. Lett. **91**, 090405 (2003).
[18] J. Åberg, D. Kult, E. Sjöqvist, and D. K. L. Oi, Phys. Rev. A **75**, 032106 (2007).
[19] A. T. Rezakhani and P. Zanardi, Phys. Rev. A **73**, 012107 (2006).
[20] J. Zhu, M. Shi, V. Vedral, X. Peng, D. Suter, and J. Du, Europhys. Lett. **94**, 20007 (2011).
[21] O. Viyuela, A. Rivas, and M. A. Martin-Delgado, Phys. Rev. Lett. **112**, 130401 (2014).
[22] F. D. M. Haldane, Phys. Rev. Lett. **61**, 2015 (1988).
[23] B. A. Bernevig, T. L. Hughes, and S.-C. Zhang, Science **314**, 1757 (2006).
[24] D. R. Hofstadter, Phys. Rev. B **14**, 2239 (1976).
[25] See Supplemental Material at http://link.aps.org/supplemental/10.1103/PhysRevLett.113.076407 for a self-contained introduction of Uhlmann's parallel transport, its relation with the Wilson Loop operator at zero temperature, and some results for two-band models..
[26] S. Pancharatnam, in *Proceedings of the Indian Academy of Sciences, Section A* (Indian Academy of Sciences, Bangalore, 1956), Vol. 44, p. 247.
[27] M. V. Berry, Proc. R. Soc. A **392**, 45 (1984).
[28] F. Wilczek and A. Zee, Phys. Rev. Lett. **52**, 2111 (1984).
[29] Z. Huang and D. P. Arovas, Phys. Rev. B **86**, 245109 (2012).
[30] R. Yu, X. L. Qi, A. Bernevig, Z. Fang, and X. Dai, Phys. Rev. B **84**, 075119 (2011).
[31] Z. Huang (unpublished).
[32] Z. Huang and D. P. Arovas, arXiv:1205.6266.
[33] At $T = 0$, $|\boldsymbol{b}_k| = 1/\sqrt{2}$, which follows from the projective nature of ρ_k (and hence $\sqrt{\rho_k}$) at $T = 0$.
[34] M. Atala, M. Aidelsburger, J. T. Barreiro, D. Abanin, T. Kitagawa, E. Demler, and I. Bloch, Nat. Phys. **9**, 795 (2013).
[35] D. A. Abanin, T. Kitagawa, I. Bloch, and E. Demler, Phys. Rev. Lett. **110**, 165304 (2013).
[36] O. Viyuela, A. Rivas, and M. A. Martin-Delgado, Phys. Rev. Lett. **113**, 076408 (2014).